

Flavonoids and cinnamic acid esters as inhibitors of fungal 17 β -hydroxysteroid dehydrogenase: A synthesis, QSAR and modelling study

Matej Sova,^a Andrej Perdih,^a Miha Kotnik,^b Katja Kristan,^c Tea Lanišnik Rižner,^c Tom Solmajer^{b,d} and Stanislav Gobec^{a,*}

^aFaculty of Pharmacy, University of Ljubljana, Aškerčeva 7, 1000 Ljubljana, Slovenia

^bLek Pharmaceuticals d.d., Drug Discovery, Verovškova 12, 1000 Ljubljana, Slovenia

^cInstitute of Biochemistry, Medical Faculty, University of Ljubljana, Vrazov trg 2, 1000 Ljubljana, Slovenia

^dNational Institute of Chemistry, Hajdrihova 19, 1001 Ljubljana, Slovenia

Received 6 March 2006; revised 3 July 2006; accepted 10 July 2006

Available online 7 August 2006

Abstract—The 17 β -hydroxysteroid dehydrogenases (17 β -HSDs) modulate the biological potency of estrogens and androgens by interconversion of inactive 17-keto-steroids and their active 17 β -hydroxy- counterparts. We have shown previously that flavonoids are potentially useful lead compounds for developing inhibitors of 17 β -HSDs. In this paper, we describe the synthesis and biochemical evaluation of structurally analogous inhibitors, the *trans*-cinnamic acid esters and related compounds. Additionally, quantitative structure–activity relationship (QSAR) and modelling studies were performed to rationalize the results and to suggest further optimization. The results stress the importance of a hydrogen bond with Asn154 and hydrophobic interactions with the aromatic side chain of Tyr212 for optimal molecular recognition.

© 2006 Elsevier Ltd. All rights reserved.

1. Introduction

Steroid hormones have important roles in the aetiology of hormone-dependent diseases, such as breast, prostate and endometrial cancer, disorders of reproduction and neuronal diseases.¹ They act via specific receptors that can activate gene transcription. The occupancy of the steroid hormone receptors is regulated mainly by hydroxysteroid dehydrogenases, which convert steroids at positions 3, 11, 17, and 20 of the steroid core, thereby acting as molecular switches.¹ The 17 β -hydroxysteroid dehydrogenases (17 β -HSDs) modulate the biological potencies of estrogens and androgens by converting inactive 17-keto-steroids into their active 17 β -hydroxy-forms (such as estradiol, testosterone, and dihydrotestosterone), or vice versa, using NAD(P)H or NAD(P)⁺, respectively (Fig. 1). Fourteen different mammalian 17 β -HSDs have been described, that belong to the protein

superfamilies of short-chain dehydrogenases/reductases (SDRs) or aldo-keto reductases (AKRs).^{2,3}

Flavonoids are polyphenolic compounds that possess estrogenic activity and have been isolated from a wide variety of plants. They are abundant in soy products, a major component of the Asian diet. The incidence of breast, prostate and endometrial cancers is much lower in Asia than in Northern Europe and USA, and it has been suggested that flavonoids could have a major impact on the development of hormone-dependent forms of cancer.^{4–6} Flavonoids comprise flavones, flavanols, flavanones, isoflavones, and chalcones,⁷ which can have antiviral, anti-inflammatory, antimutagenic and anticarcinogenic activities.⁸ The influence of flavonoids has been studied on steroid metabolizing enzymes. They inhibit aromatase, sulfatase, sulfotransferase, 5 α -reductase, 3 β -HSD Δ 5/ Δ 4 isomerase, 11 β -HSD type 1 and type 2 and 17 β -HSDs.^{8–14} Flavonoids have been shown to inhibit human 17 β -HSD types 1, 2, 3, and 5,^{15–22} as well as 17 β -HSD from the fungus *Cochliobolus lunatus* (17 β -HSDcl), a model enzyme of the SDR superfamily.²³

Keywords: 17 β -Hydroxysteroid dehydrogenases; Inhibitors; Molecular modelling; Anticancer agents.

* Corresponding author. Tel.: +386 1 47 69 585; fax: +386 1 42 58 031; e-mail: gobecs@ffa.uni-lj.si

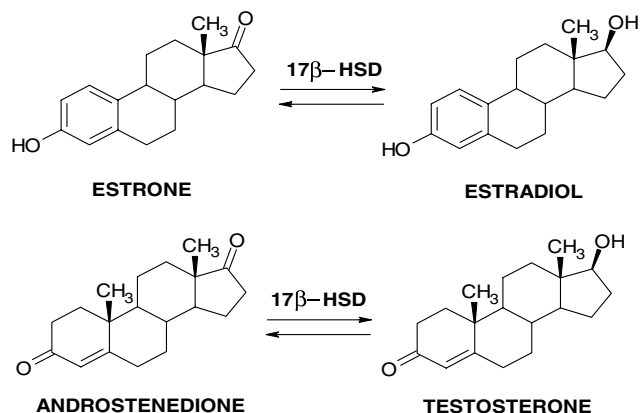


Figure 1. Reactions catalyzed by 17β -hydroxysteroid dehydrogenases.

Over the last decade, considerable attention has been devoted to the search for inhibitors of type 1 17β -HSD, which is a very promising target for the development of new drugs for treating breast cancer.²²

Flavonoids are thus potentially useful lead compounds for developing inhibitors of 17β -HSDs. Their biosynthesis in plants proceeds via *trans*-cinnamic acid and related phenolic acids like caffeic acid, ferulic acid and chlorogenic acid.²⁴ We have therefore focused on the synthesis and biochemical evaluation of *trans*-cinnamic acid esters and related compounds, since their structures are similar to those of flavones and chalcones. We have synthesized an initial series of *trans*-cinnamic acid esters and coumarin-3-carboxylates of general formulae of **I** and **II**, respectively (Fig. 2), and have reported in a preliminary communication that some of these compounds inhibit fungal 17β -HSD.²⁵

In the present study, we describe the synthesis and inhibitory activities of a more extended series of 17β -HSDcl inhibitors. Additionally, a quantitative structure–activity relationship (QSAR) study was performed on the complete series of flavonoids²⁶ and related compounds synthesized in our laboratory, providing important information for rapid optimization of lead candidates. Docking studies were also used to model 17β -HSDcl–ligand interactions, to rationalize the results of the

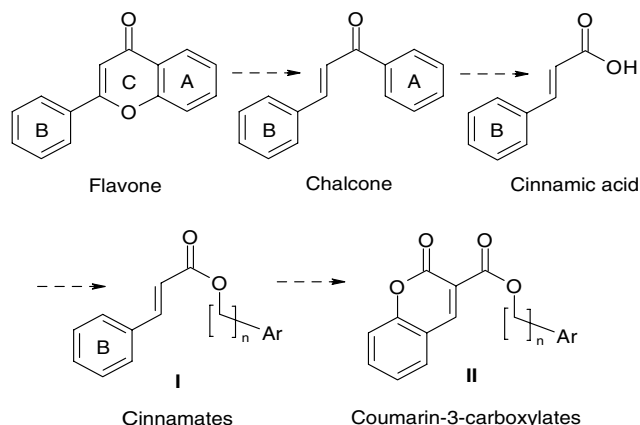


Figure 2. Design of synthetic inhibitors of 17β -HSDs (Ar, aromatic; $n = 0$ –2).

QSAR analyses and to suggest further directions for the design of new inhibitors.

2. Results and discussion

2.1. Synthesis

Target compounds of general formulae **I** and **II** (Fig. 2) were synthesized from the corresponding carboxylic acids and alcohols or phenols. For the formation of an ester bond, we used DCC²⁷ or BOP²⁸ mediated esterification, which both gave satisfactory yields.

2.2. Biological evaluations

To evaluate the inhibitory potentials towards human type 1 17β -HSD of the compounds reported in this study, we screened their activity on 17β -HSD from the fungus *Cochliobolus lunatus* (17β -HSDcl).²⁹ This readily available fungal enzyme allows preliminary screening of compounds in a rapid and low-cost spectrophotometric assay, while the inhibitor testing with human 17β -HSD is based on use of more demanding radioactive ligands.^{30,31} We have recently shown that the flavonoids inhibit 17β -HSDcl.²³ The structural features of these flavonoids are similar to those reported for phytoestrogen inhibitors of human type 1 17β -HSD, suggesting that fungal 17β -HSD can be used as a model enzyme for the human isoform 1.²³ We have confirmed this hypothesis by a superposition and docking study (Section 2.4), which provides further evidence that the active sites of both of these enzymes share significant similarity.

2.3. QSAR model and its interpretation

Molecular descriptors collected from the derived QSAR equations are summarized in Table 1. The best QSAR model, according to the r^2 , s^2 , F test, and r_{cv}^2 values for the oxidative reaction, was obtained with a combination of one geometrical and three quantum-chemical descriptors. The QSAR model describing the inhibition of the reductive reaction consists of quantum-chemical descriptors only.

Eq. 1 presents the best QSAR model for the oxidation direction. The resulting correlation between experimental

Table 1. Specification of descriptors used in the derived 4-parameter QSAR models, along with the t test values for all of the descriptors (g—geometrical, q—quantum-chemical descriptors)

Descriptor	Definition	t -test
Eq. 1.	Inhibition of oxidation pathway	
D ₁	Min. exchange energy for a C–H bond ^q	5.21
D ₂	Min. e–n attraction for a C–O bond ^q	4.01
D ₃	Principal moment of inertia A/# of atoms ^g	–2.94
D ₄	Max bond order of a H atom ^q	4.59
Eq. 2.	Inhibition of reduction pathway	
D ₅	Max electroph. react. index for an O atom ^q	6.76
D ₆	Min. exchange energy for a C–H bond ^q	4.31
D ₇	Min. atomic state energy for a C atom ^q	–4.27
D ₈	Max 1-electron react. index for a C atom ^q	3.16

and calculated biological activities for all of the treated compounds is summarized in Table 2. A detailed analysis of Table 2 reveals that the model obtained is able to predict almost all of the inhibitory activities within one order of magnitude for compounds comprising the training set. It is of note that the model (Eq. 1) consists of only orthogonal descriptors, as shown in Table 3.

$$\begin{aligned} \log(1/IC_{50}) = & (1.75 \times 10^1 \pm 3.62) \cdot \mathbf{D}_1 \\ & + (1.51 \times 10^{-1} \pm 3.76 \times 10^{-2}) \cdot \mathbf{D}_2 \\ & - (4.18 \times 10^2 \pm 1.42 \times 10^2) \cdot \mathbf{D}_3 \\ & - (7.41 \times 10^1 \pm 1.61 \times 10^1) \cdot \mathbf{D}_4 \\ & - (7.42 \times 10^1 \pm 2.59 \times 10^1) \end{aligned} \quad (1)$$

$$N = 33, r = 0.867, F = 21.11, s^2 = 0.5073, r_{cv}^2 = 0.6302$$

The most important test of the model is its ability to correctly predict the biological activities of compounds in the external validation set that were not included in the QSAR model development.³² In Table 2, all of the structures in the corresponding external validation set are indicated by an asterisk. The results are presented graphically in Figure 3.

Analysis of the information content of the descriptors allows further conclusions to be drawn. The most important descriptor is the minimum exchange energy for a C–H bond. This energy reflects the change in the Fermi correlation energy between the two electrons localized on the C and H atoms. It can be significant in determining the conformational changes of the molecule and its spin properties. The principal moment of inertia A (\mathbf{D}_3) is a geometric descriptor that characterizes the mass distribution in the molecule. Examination of the structures in Table 2 reveals that several aromatic centres are present in both chemical subtypes. The aromatic regions of the molecules can be considered to contribute significantly to the binding affinity through hydrophobic interactions.

Eq. 2 shows the QSAR model derived for the inhibition of reduction. The resulting statistical characteristics of this model are good, with prediction ability even slightly better than in the case of Eq. 1. Values of experimental and calculated inhibitory activities are summarized in Table 2. The correlation matrix presented in Table 3 indicates that Eq. 2 is comprised of orthogonal descriptors only.

$$\begin{aligned} \log(1/IC_{50}) = & (2.39 \times 10^2 \pm 3.54 \times 10^1) \cdot \mathbf{D}_5 \\ & + (1.22 \times 10^1 \pm 2.85) \cdot \mathbf{D}_6 \\ & - (2.32 \pm 5.43 \times 10^{-1}) \cdot \mathbf{D}_7 \\ & + (5.19 \times 10^1 \pm 1.64) \cdot \mathbf{D}_8 \\ & - (1.71 \times 10^2 \pm 5.36 \times 10^1) \end{aligned} \quad (2)$$

$$N = 30, r = 0.885, F = 22.79, s^2 = 0.3508, r_{cv}^2 = 0.6942$$

The predictive power of the second QSAR model (Eq. 2, Fig. 4) was evaluated with an external validation set,

which comprised the six molecules underlined in Table 2.

The QSAR models developed exhibit a reasonable ability to predict biological activity. Six out of seven compounds in the external prediction set for the oxidation direction, and five out of six compounds for the reduction direction are predicted within one order of magnitude. Compounds **11** and **24**, however, were somewhat less accurately predicted, with errors of 2.4 and 1.6 log units, respectively.

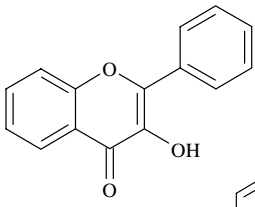
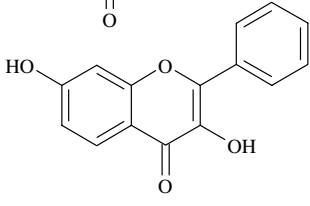
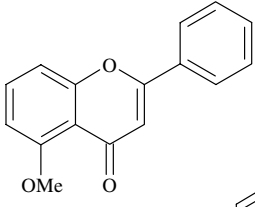
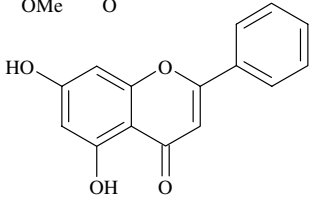
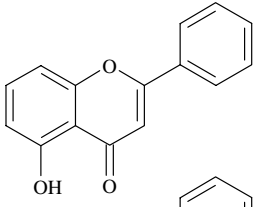
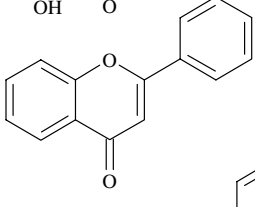
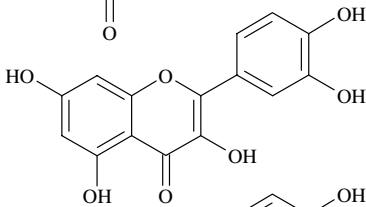
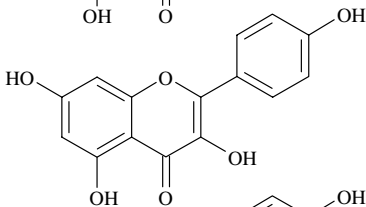
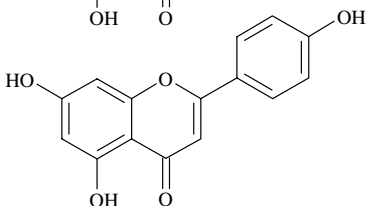
2.4. Proposed binding modes of flavones and *trans*-cinnamic acid esters in the type 1 17 β -HSD and 17 β -HSDcl active site

Flexible docking experiments were carried out to identify the possible binding modes of the *trans*-cinnamic acid esters and flavone type inhibitors into the 17 β -HSDcl active site.³³ As in our previous molecular docking studies of flavone type inhibitors, it was necessary to use a homology built model³⁴ of 17 β -HSDcl, supported by preliminary crystallographic data,³⁵ with added coenzyme NADPH, since inhibitory activities were determined using this enzyme.²³ Sequence identity between the 17 β -HSDcl and human type 1 17 β -HSD is relatively low.²³ However, despite low sequence homology of 25–30% between the different types of 17 β -HSDs, the enzymes of the SDR family share a very common protein fold with several conserved motifs.³⁶ As shown in Figure 5, the positions of the catalytical residues in fungal 17 β -HSD (Tyr167, Ser153, and Lys171) are conserved with the positions of the catalytical triad of 17 β -HSD type 1 (Tyr155, Ser142, and Lys159) (RMS = 0.66). The secondary structures of the β sheets and helix delineating the inhibitor binding site (red and green ribbons represent the protein backbone) are remarkably similar. Two hydrogen bonds between the 3-hydroxyl group and the 4-carbonyl of inhibitor **1** and Asn154 are shown, along with the Tyr212 residue of 17 β -HSDcl. These two residues which appear crucial for binding of inhibitors in the fungal enzyme active site could be matched by their counterparts Arg258 and Tyr218 of human type 1 17 β -HSD enzyme. Also, the cofactor NADP in both enzymes occupies the same position (shown in part in Fig. 5).

In principle, the results of the docking studies are dependent on the oxidation state of the coenzyme. However, as in our previous studies, we found that the binding mode of the inhibitors did not change significantly if different charges were assigned to the coenzyme, in the inhibition of both oxidation and reduction pathways.²³ Therefore, the binding mode in this study was evaluated for the coenzyme in the oxidation state, as determined experimentally.

The representative docked conformation of flavone type inhibitor **1** is depicted in Figure 5. A relatively uniform binding mode and similar conformations were observed on superimposing the 30 docked conformations with lowest energy of binding to the enzyme active site. The carbonyl oxygen and a ring hydroxyl group of **1** both

Table 2. Summary of calculated and experimental (Eqs. 1 and 2.) biological activities (Δ represents the difference between the two) of non-steroidal inhibitors of 17 β -hydroxysteroid dehydrogenase (oxidation and reduction directions) in log scale along with the original IC₅₀ values

Compound	Structure	IC ₅₀ (μ M) _{oxidn}	log ^{calcd} (1/IC ₅₀) _{oxidn}	log ^{exp.} (1/IC ₅₀) _{oxidn}	Δ_{oxidn}
		IC ₅₀ (μ M) _{redn}	log ^{calcd} (1/IC ₅₀) _{redn}	log ^{exp.} (1/IC ₅₀) _{redn}	Δ_{redn}
1		0.4	6.131	6.398	-0.267
		1.2	5.878	5.921	-0.043
2		0.6	6.068	6.222	-0.154
		6.0	5.596	5.222	0.374
3		0.7	4.857	6.155	-1.298
		2.0	4.429	5.698	-1.269
4		0.9	5.680	6.046	-0.366
		7.4	5.060	5.131	-0.071
5*		1.0	5.646	6.000	-0.354
		4.8	5.018	5.319	-0.301
6		1.3	5.616	5.886	-0.270
		8.0	4.679	5.096	-0.417
7		2.0	6.065	5.698	0.367
		7.7	5.659	5.113	0.546
8		2.5	6.119	5.602	0.517
		3.9	5.453	5.409	0.044
9		2.9	5.988	5.538	0.450
		54.0	4.928	4.268	0.660

(continued on next page)

Table 2 (continued)

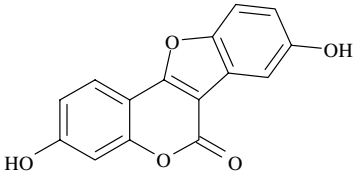
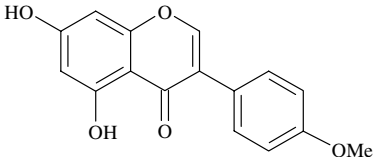
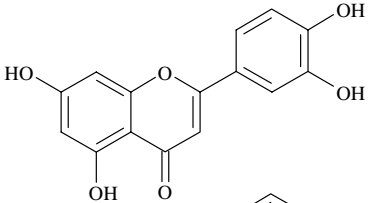
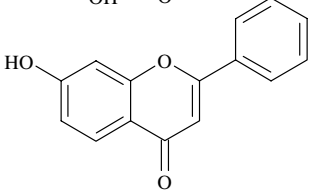
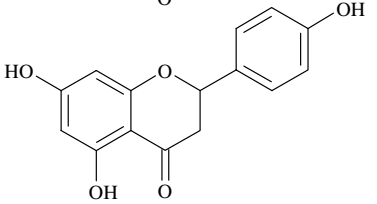
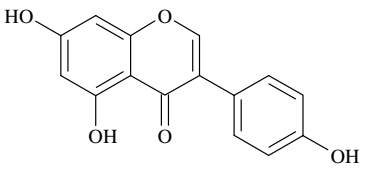
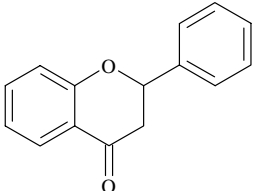
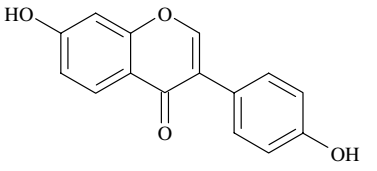
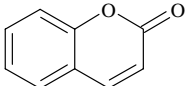
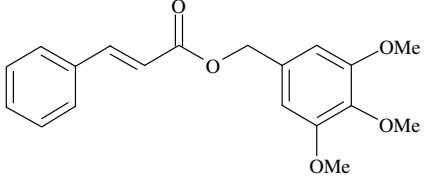
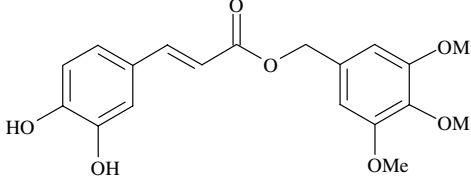
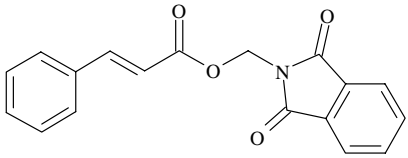
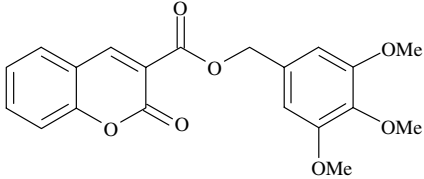
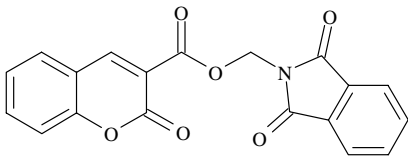
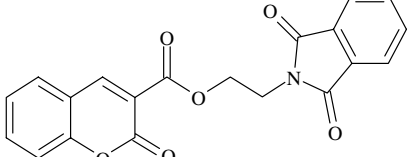
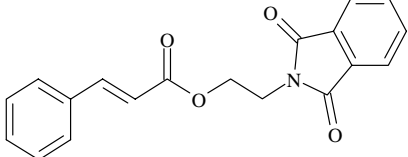
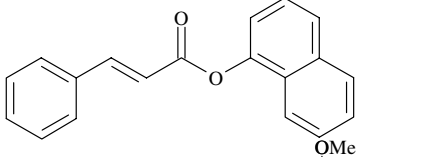
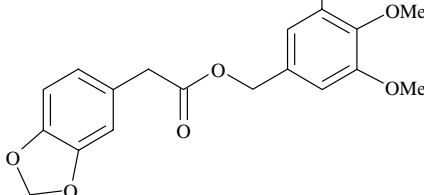
Compound	Structure	$IC_{50}(\mu M)_{oxidn}$	$\log^{calcd}(1/IC_{50})_{oxidn}$	$\log^{exp.}(1/IC_{50})_{oxidn}$	Δ_{oxidn}
		$IC_{50}(\mu M)_{redn}$	$\log^{calcd}(1/IC_{50})_{redn}$	$\log^{exp.}(1/IC_{50})_{redn}$	Δ_{redn}
10		3.2	4.672	5.495	-0.823
		2.8	5.265	5.553	-0.288
11*		7.3	2.891	5.267	-2.376
		11.5	4.246	4.939	-0.693
12*		10.5	5.889	4.978	0.911
		20.0	4.831	4.699	0.132
13		15.0	5.725	4.824	0.901
		50.0	4.734	4.301	0.433
14		17.3	3.619	4.762	-1.143
		31.8	3.526	4.498	-0.972
15		225.0	3.754	3.648	0.106
		56.0	4.287	4.252	0.035
16		227.0	3.462	3.644	-0.182
		273.0	3.567	3.564	0.003
17		301.0	3.868	3.521	0.347
		408.0	4.271	3.389	0.882
18		>3000	2.956	2.523	0.433
		>3000	3.179	2.523	0.656

Table 2 (continued)

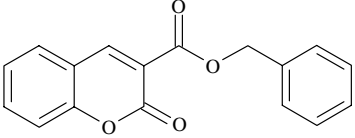
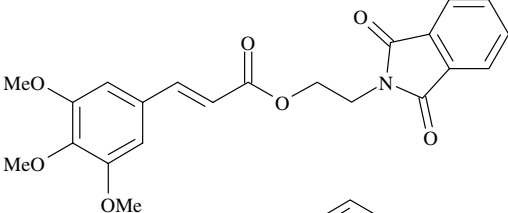
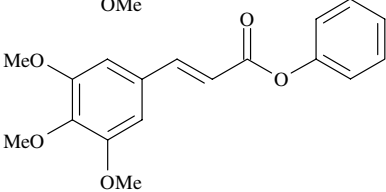
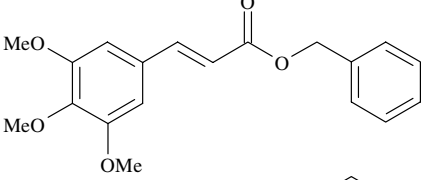
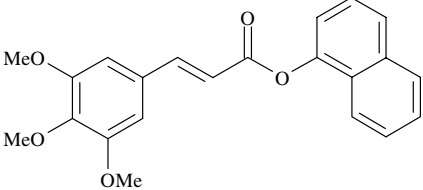
Compound	Structure	$IC_{50}(\mu M)_{oxidn}$	$\log^{calcd}(1/IC_{50})_{oxidn}$	$\log^{exp.}(1/IC_{50})_{oxidn}$	Δ_{oxidn}
		$IC_{50}(\mu M)_{redn}$	$\log^{calcd}(1/IC_{50})_{redn}$	$\log^{exp.}(1/IC_{50})_{redn}$	Δ_{redn}
19		14.0 >3000	4.318 —	4.854 2.523	-0.536 —
20		48.0 >3000	4.303 2.629	4.319 2.523	-0.016 0.106
21		10.0 >3000	3.679 2.963	5.000 2.523	-1.321 0.440
22		>3000 >3000	2.156 2.302	2.523 2.523	-0.367 -0.221
23		>3000 >3000	2.814 2.603	2.523 2.523	0.291 0.080
24		5.0 90.0	3.673 4.162	2.523 2.523	1.150 1.639
25		10.0 470.2	4.990 3.767	5.301 4.046	-0.311 -0.279
26		>3000 >3000	5.117 3.227	5.000 3.328	0.117 -0.101
27		>3000 NA	2.799 —	2.523 NA	0.277 —

(continued on next page)

Table 2 (continued)

Compound	Structure	IC ₅₀ (μM) _{oxidn}	log ^{calcd} (1/IC ₅₀) _{oxidn}	log ^{exp} : (1/IC ₅₀) _{oxidn}	Δ _{oxidn}
		IC ₅₀ (μM) _{redn}	log ^{calcd} (1/IC ₅₀) _{redn}	log ^{exp} : (1/IC ₅₀) _{redn}	Δ _{redn}
28		>3000 NA	2.911 —	2.523 NA	0.388 —
29		0.7 7.3	5.147 3.808	6.155 5.137	-1.008 -1.329
30		26.0 310.0	4.446 3.462	4.585 3.509	-0.139 -0.047
31		130.0 >3000	5.387 2.574	3.886 2.523	1.501 0.051
32		13.0 >3000	4.459 —	4.886 2.523	-0.427 —
33*		400.0 1500	2.929 2.768	3.398 2.824	-0.469 -0.056
34		135.0 >3000	4.046 3.230	3.870 2.523	0.176 0.707
35		2500 2500	2.838 2.767	2.602 2.602	0.236 0.165
36		>3000 >3000	3.388 3.356	2.523 2.523	0.865 0.833

Table 2 (continued)

Compound	Structure	$IC_{50}(\mu M)_{oxidn}$	$\log^{calcd}(1/IC_{50})_{oxidn}$	$\log^{exp.}(1/IC_{50})_{oxidn}$	Δ_{oxidn}
		$IC_{50}(\mu M)_{redn}$	$\log^{calcd}(1/IC_{50})_{redn}$	$\log^{exp.}(1/IC_{50})_{redn}$	Δ_{redn}
37		2.7	—	5.569	—
		7.6	—	5.119	—
<u>38*</u>		57.4	4.077	4.241	-0.164
		283.7	3.768	3.547	0.221
<u>39*</u>		63.9	4.166	4.194	-0.028
		25.9	3.738	4.586	-0.849
40*		10.8	4.367	4.967	-0.600
		144	3.729	3.842	-0.113
41		159.5	4.298	3.797	0.501
		>3000	3.110	2.523	0.587

Underlined (reduction path) and asterisk-marked (oxidation path) compounds constitute the corresponding external prediction (validation) sets. NA, not available.

Table 3. Correlation matrices for the descriptors presented in Eqs. 1 and 2

	Eq. 1			
	D ₁	D ₂	D ₃	D ₄
D ₁	1			
D ₂	0.2112	1		
D ₃	0.2961	-0.0973	1	
D ₄	-0.1155	-0.0429	-0.2358	1
	Eq. 2			
	D ₅	D ₆	D ₇	D ₈
D ₅	1			
D ₆	0.0497	1		
D ₇	0.3991	0.2578	1	
D ₈	-0.0497	0.1299	0.2991	1

form stable hydrogen bonds with Asn154. The π - π interaction between the benzene ring B of the flavone **1** and Tyr212 makes a major contribution to the binding. Analysis of the enzyme-inhibitor complex highlights other amino-acid residues in the active site that can form hydrophobic interactions, such as Val161

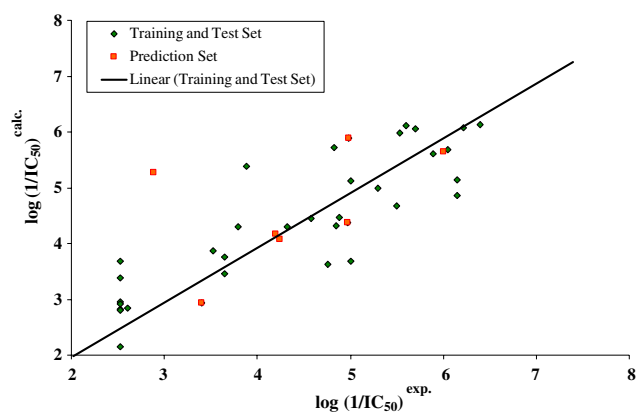


Figure 3. Correlation between experimental inhibitory activities of non-steroidal inhibitors of 17 β -hydroxysteroid dehydrogenase (oxidation reaction) and those predicted by Eq. 1.

and Ala269. This underlines that favourable interplay between properly oriented hydrogen bonds and elements in the structure that form hydrophobic interactions is crucial for optimal molecular recognition. A similar

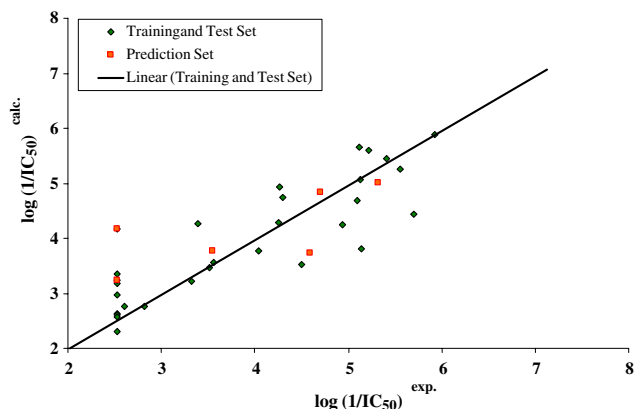


Figure 4. Correlation between experimental inhibitory activities of non-steroidal inhibitors of 17 β -hydroxysteroid dehydrogenase (reduction reaction) and those predicted by Eq. 2.

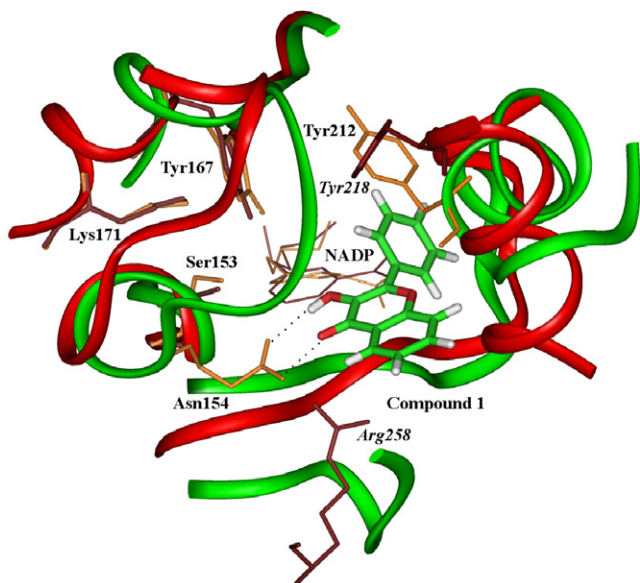


Figure 5. Representative conformation of **1** in the active site of 17 β -HSDcl (green) and type 1 17 β -HSD (red). Residues Arg258 and Tyr212 of the human enzyme are marked in italic. Cofactor NADP is shown just in part for clarity.

binding mode was observed during our previous studies that used a more simplified docking approach.²³ Ring B is positioned slightly differently with respect to the conformation of flavonoids described previously.²³ However, the energy difference for torsion angle rotation is relatively low.

A similar situation is seen for the *trans*-cinnamic acid ester **29**. The conformations proposed by the FlexX molecular docking tool are strikingly uniform with respect to the RMS between the conformers. At the same time, their position in the active site points to a significant interaction—a hydrogen bond between Asn154 and the ester carbonyl oxygen. In addition, the hydrophobic and π – π interactions between the phenyl B rings of compound **29** and Tyr212 also contribute to the optimal binding pattern proposed in Figure 6. The amino-acid residues of the catalytic triad, Tyr167, Ser153,

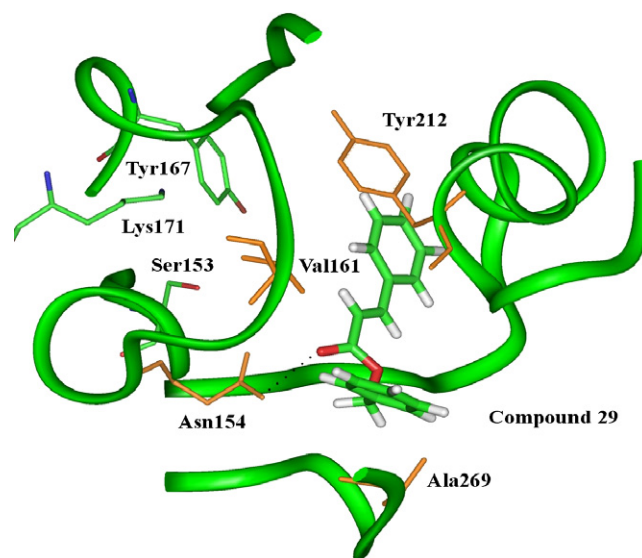


Figure 6. Conformation of **29** in the active site of 17 β -HSDcl. The hydrogen bond between the carbonyl of the inhibitor and Asn154 is shown, together with the amino-acid residues of the 17 β -HSDcl active site that form hydrophobic interactions.

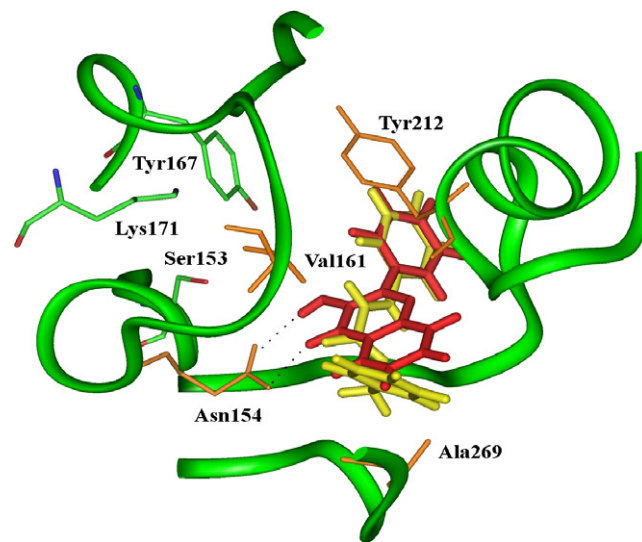


Figure 7. Comparison of the binding modes of flavone type inhibitor **1** (red) and *trans*-cinnamic acid ester **29** (yellow).

and Lys171, are adjacent to the binding site of the inhibitors in our series.

The superposition of compounds **1** and **29** in the 17 β -HSDcl active site is outlined in Figure 7. Compound **1** forms two hydrogen bonds, although its inhibitory activity is only slightly higher than that measured for compound **29**.

3. Conclusions

Based on the flavonoid inhibitors of 17 β -HSDcl, a series of structurally related cinnamates and coumarin-3-carboxylates were designed, synthesized and evaluated for

their inhibitory activities. QSAR models for both oxidative and reductive reactions catalyzed by 17 β -HSDcl were developed, and the experimental inhibitory activities show the importance of the binding of the carbonyl group on the chromone and cinnamoyl moieties, as well as hydrophobic structural elements. These results are further supported by the studies of docking into the 17 β -HSDcl active site, which stress the importance of a putative hydrogen bond to Asn154 and hydrophobic interactions with the aromatic side chain of Tyr212 for optimal molecular recognition. As the 17 β -HSD from the fungus *Cochliobolus lunatus* may serve as a model enzyme for the human type 1 17 β -HSD, the most strongly inhibitory compounds described in this study represent promising hits for the development of inhibitors of human enzyme.

4. Experimental

4.1. Chemistry

All chemicals were obtained from commercial sources (Acros, Aldrich, Fluka, Merck, Janssen, and Sigma) and used without further purification. Solvents were used without purification or drying, unless otherwise stated. Reactions were monitored using analytical TLC plates (Merck, silica gel 60 F₂₅₄) with rhodamin G6 or sulfuric acid staining. Silica gel grade 60 (70–230 mesh, Merck) was used for column chromatography. NMR spectra were obtained on a Bruker Avance DPX 300 instrument. ¹H NMR were recorded at 300.13 MHz with tetramethylsilane as an internal standard. Mass spectra were obtained with a VG-Analytical Autospec Q mass spectrometer with EI or FAB ionization (MS Centre, Jožef Stefan Institute, Ljubljana). IR spectra were recorded on a Perkin-Elmer FTIR 1600 spectrometer. Elemental analyses were carried out by the Department of Organic Chemistry, Faculty of Chemistry and Chemical Technology, Ljubljana, on a Perkin-Elmer elemental analyzer 240 C. Melting points were determined using a Reichert hot-stage microscope and are uncorrected.

4.2. General method for esterification using DCC (method A)

To a stirred solution of the appropriate acid (5 mmol) and alcohol (5.5 mmol) in dichloromethane (25 mL), DCC (5.5 mmol) and DMAP (0.5 mmol) were added. After 24 h stirring at room temperature, the reaction mixture was filtered and the solution washed with 10% citric acid (2 \times 20 ml), water (15 ml), and brine (30 ml), dried over anhydrous sodium sulfate, filtered and concentrated under reduced pressure. The crude product was purified by column chromatography or crystallized from the appropriate solvent.

4.3. General method for esterification using BOP reagent (method B)

To a stirred solution of the appropriate acid (5 mmol) and alcohol (5.5 mmol) in dichloromethane (25 ml),

BOP (6 mmol) and triethylamine (20 mmol) were added. After 24 h stirring at room temperature, dichloromethane was removed under reduced pressure and ethyl acetate (80 ml) was added to the residual reaction mixture. The resulting solution was washed with 10% citric acid (2 \times 40 ml), 10% solution of NaHCO₃ (3 \times 40 ml), water (40 ml) and brine (2 \times 40 ml), dried over anhydrous sodium sulfate, filtered and concentrated under reduced pressure. The crude product was purified by column chromatography or crystallized from the appropriate solvent.

4.3.1. (*E*)-3,4,5-Trimethoxybenzyl cinnamate (19). This compound was prepared from *trans*-cinnamic acid and (3,4,5-trimethoxyphenyl)methanol by method B, and crystallized from hexane as white needles. Yield 13%; mp 85–86 °C; IR (KBr): ν_{\max} 2936, 2834, 1710, 1638, 1593, 1508, 1423, 1332, 1245, 1124, 971, and 858 cm⁻¹; ¹H NMR (300 MHz, DMSO-*d*₆): δ (ppm) 3.87 (s, 3H, OCH₃), 3.90 (s, 6H, 2 \times OCH₃), 5.20 (s, 2H, CH₂), 6.51 (d, *J* = 16.0 Hz, 1H, CH=CH-CO), 6.66 (s, 2H, aromatic), 7.38–7.45 (m, 3H, aromatic), 7.50–7.75 (m, 2H, aromatic), 7.76 (d, *J* = 16.0 Hz, 1H, CH=CH-CO); FAB MS *m/z* 328 (M+H)⁺; Anal. Calcd for C₁₉H₂₀O₅·0.33H₂O: C, 68.25; H, 6.23. Found: C, 68.35; H, 6.21.

4.3.2. (*E*)-3,4,5-Trimethoxybenzyl 3-(3,4-dihydroxyphenyl)acrylate (20). This compound was prepared from (*E*)-3-(3,4-dihydroxyphenyl)acrylic acid and (3,4,5-trimethoxyphenyl)methanol by method B, as a yellow solid. Yield 18%; mp 98–99 °C; IR (KBr): ν_{\max} 2940, 1595, 1511, 1466, 1357, 1240, 1132, 1004, 929, 827, and 734 cm⁻¹; ¹H NMR (300 MHz, DMSO-*d*₆): δ (ppm) 3.75 (s, 6H, 2 \times OCH₃), 3.80 (s, 3H, OCH₃), 5.48 (s, 2H, CH₂), 6.48 (s, 2H, aromatic), 7.16 (d, *J* = 15.8 Hz, 1H, CH=CH-CO), 7.29–7.41 (m, 3H, aromatic), 7.98 (d, *J* = 15.8 Hz, 1H, CH=CH-CO); EI MS *m/z* 360 (M). Anal. Calcd for C₁₉H₂₀O₇·0.75H₂O: C, 61.04; H, 5.80. Found: C, 60.80; H, 5.49.

4.3.3. (*E*)-(1,3-Dioxoisindolin-2-yl)methyl 3-(3,4,5-trimethoxyphenyl)acrylate (21). This compound was prepared from *trans*-cinnamic acid and 2-(hydroxymethyl)isindoline-1,3-dione by method B, and crystallized from hexane as a white solid. Yield 12%; mp 146–147 °C; IR (KBr): ν_{\max} 2974, 1728, 1633, 1434, 1304, 1136, 976, 856, 711, and 616 cm⁻¹; ¹H NMR (300 MHz, DMSO-*d*₆): δ (ppm) 5.89 (s, 2H, CH₂), 6.42 (d, *J* = 16.0 Hz, 1H, CH=CH-CO), 7.35–7.43 (m, 3H, aromatic), 7.50–7.56 (m, 2H, aromatic), 7.74 (d, *J* = 16.0 Hz, 1H, CH=CH-CO), 7.80–7.86 (m, 2H, aromatic), 7.95–8.05 (m, 2H, aromatic); FAB MS *m/z* 308 (M+H)⁺; Anal. Calcd for C₁₈H₁₃NO₄: C, 70.36; H, 4.23; N, 4.56. Found: C, 70.03; H, 4.23; N, 4.52.

4.3.4. 3,4,5-Trimethoxybenzyl 2-oxo-2H-chromene-3-carboxylate (22). This compound was prepared from 2-oxo-2H-chromene-3-carboxylic acid and (3,4,5-trimethoxyphenyl)methanol by method B, and recrystallized from ethyl acetate as a reddish-white solid. Yield 49%; mp 145–146 °C; IR (KBr): ν_{\max} 2937, 1741, 1709, 1612,

1566, 1509, 1457, 1372, 1307, 1128, 1008, 793, and 584 cm^{-1} ; ^1H NMR (300 MHz, DMSO- d_6): δ (ppm) 3.86 (s, 3H, OCH₃), 3.96 (s, 6H, 2 \times OCH₃), 5.36 (s, 2H, CH₂), 6.78 (s, 2H, aromatic), 7.25–7.32 (m, 2H, aromatic), 7.60–7.66 (m, 2H, aromatic), 8.48 (s, 1H, CH=C); FAB MS m/z 370 (M+H)⁺; Anal. Calcd for C₂₀H₁₈O₇: C, 64.86; H, 4.86. Found: C, 64.75; H, 4.91.

4.3.5. (1,3-Dioxoisindolin-2-yl)methyl 2-oxo-2H-chromene-3-carboxylate (23). This compound was prepared from 2-oxo-2H-chromene-3-carboxylic acid and 2-(hydroxymethyl)isoindoline-1,3-dione by method B, and crystallized from hexane as a white solid. Yield 52%; mp 240–243 °C; IR (KBr): ν_{max} 3052, 1759, 1717, 1612, 1563, 1409, 1301, 1243, 969, and 770 cm^{-1} ; ^1H NMR (300 MHz, DMSO- d_6): δ (ppm) 6.00 (s, 2H, CH₂), 7.25–7.40 (m, 2H, aromatic), 7.55–7.72 (m, 2H, aromatic), 7.78–7.88 (m, 2H, aromatic), 7.92–8.05 (m, 2H, aromatic), 8.53 (s, 1H, CH=C); EI MS m/z 349 (M); Anal. Calcd for C₁₉H₁₁NO₆·0.25H₂O: C, 64.50; H, 3.28; N, 3.96. Found: C, 64.31; H, 3.10; N, 4.09.

4.3.6. 2-(1,3-Dioxoisindolin-2-yl)ethyl 2-oxo-2H-chromene-3-carboxylate (24). This compound was prepared from 2-oxo-2H-chromene-3-carboxylic acid and 2-(2-hydroxyethyl)isoindoline-1,3-dione by method B, as a white solid. Yield 10%; mp 193–196 °C; IR (KBr): ν_{max} 3082, 2961, 1763, 1714, 1608, 1567, 1427, 1245, 1017, and 722 cm^{-1} ; ^1H NMR (300 MHz, CDCl₃): δ (ppm) 4.10 (t, J = 5.3 Hz, 2H, CH₂N), 4.60 (t, J = 5.3 Hz, 2H, OCH₂), 7.31–7.38 (m, 2H, aromatic), 7.61–7.67 (m, 2H, aromatic), 7.71–7.76 (m, 2H, aromatic), 7.84–7.89 (m, 2H, aromatic), 8.55 (s, 1H, CH=C); EI MS m/z 363 (M); Anal. Calcd for C₂₀H₁₃NO₆: C, 66.10; H, 3.58; N, 3.86. Found: C, 66.46; H, 3.29; N, 3.70.

4.3.7. (E)-2-(1,3-Dioxoisindolin-2-yl) ethyl cinnamate (25). This compound was prepared from *trans*-cinnamic acid and 2-(2-hydroxyethyl) isoindoline-1,3-dione by method A, as a white solid. Yield 45%; mp 115–118 °C; IR (KBr): ν_{max} 2929, 2119, 1777, 1708, 1627, 1428, 1392, 1320, 1255, 1202, 1067, 1016, 866, and 723 cm^{-1} ; ^1H NMR (300 MHz, CDCl₃): δ (ppm) 4.07 (t, J = 5.3 Hz, 2H, CH₂), 4.47 (t, J = 5.3 Hz, 2H, CH₂), 6.39 (d, J = 15.8 Hz, 1H, CH=CH-CO), 7.34–7.43 (m, 3H, aromatic), 7.47–7.57 (m, 2H, aromatic), 7.68 (d, J = 15.8 Hz, 1H, CH=CH-CO), 7.72–7.78 (m, 2H, aromatic), 7.84–7.93 (m, 2H, aromatic); FAB MS m/z 322 (M+H)⁺; Anal. Calcd for C₁₉H₁₅NO₄·0.25H₂O: C, 70.04; H, 4.79; N, 4.30. Found: C, 70.20; H, 5.25; N, 4.59.

4.3.8. (E)-1-Naphthyl cinnamate (26). This compound was prepared from *trans*-cinnamic acid and 1-naphthol by method A, as a brown solid. Yield 20%; mp 105–108 °C; IR (KBr): ν_{max} 3042, 1723, 1629, 1449, 1310, 1134, 1014, 865, 767, and 684 cm^{-1} ; ^1H NMR (300 MHz, CDCl₃): δ (ppm) 6.84 (d, J = 16.0 Hz, 1H, CH=CH-CO), 7.34–7.39 (m, 1H, aromatic), 7.44–7.51 (m, 3H, aromatic), 7.51–7.58 (m, 3H, aromatic), 7.63–7.71 (m, 2H, aromatic), 7.79 (d, J = 8.3 Hz, 1H, aromatic), 7.88–7.99 (m, 2H, aromatic), 7.99–8.06 (d, J = 16.0 Hz, 1H, CH=CH-CO); FAB MS m/z 275

(M+H)⁺; Anal. Calcd for C₁₉H₁₄O₂: C, 83.19; H, 5.14. Found: C, 83.31; H, 5.35.

4.3.9. 3,4,5-Trimethoxybenzyl 2-(benzo[*d*][1,3] dioxol-6-yl)acetate (27). This compound was prepared from 2-(benzo[*d*][1,3]dioxol-5-yl)acetic acid and (3,4,5-trimethoxyphenyl)methanol by method B, as a colourless oil. Yield 10%; IR (KBr): ν_{max} 2490, 1734, 1593, 1491, 1446, 1333, 1247, 1129, 1038, 929, and 812 cm^{-1} ; ^1H NMR (300 MHz, CDCl₃): δ (ppm) 3.60 (s, 2H, CH₂-CO), 3.85 (s, 9H, 3 \times OCH₃), 5.10 (s, 2H, O-CH₂), 5.95 (s, 2H, O-CH₂-O) 6.50 (s, 2H, aromatic), 6.75–6.77 (m, 2H, aromatic), 6.82 (s, 1H, aromatic); EI MS m/z 360 (M); Anal. Calcd for C₁₉H₂₀O₇·0.75H₂O: C, 61.04; H, 5.80. Found: C, 60.87; H, 5.60.

4.3.10. (1,3-Dioxoisindolin-2-yl)methyl 2-(benzo[*d*][1,3]dioxol-6-yl)acetate (28). This compound was prepared from 2-(benzo[*d*][1,3]dioxol-5-yl)acetic acid and 2-(hydroxymethyl)isoindoline-1,3-dione by method B, and crystallized from ethyl acetate as a white solid. Yield 40%; mp 126–129 °C; IR (KBr): ν_{max} 3483, 2914, 1784, 1715, 1492, 1405, 1240, 1131, 978, 800, and 724 cm^{-1} ; ^1H NMR (300 MHz, CDCl₃): δ (ppm) 3.55 (s, 2H, CH₂-CO), 5.75 (s, 2H, CH₂-N), 5.95 (s, 2H, O-CH₂-O), 6.67–6.80 (m, 3H, aromatic), 7.76–7.84 (m, 2H, aromatic), 7.90–7.98 (m, 2H, aromatic); EI MS m/z 339 (M); Anal. Calcd for C₁₈H₁₃NO₆: C, 63.70; H, 3.83; N, 4.13. Found: C, 63.35; H, 3.98; N, 4.38.

4.3.11. (E)-Benzyl cinnamate (29). This compound was prepared from *trans*-cinnamic acid and benzyl alcohol by method A, as white crystals. Yield 79%; mp 33–35 °C, (lit.³⁷ mp 33–33.5 °C); IR (KBr): ν_{max} 3029, 1709, 1638, 1495, 1450, 1372, 1312, 1161, 981, 905, 755, 697, and 527 cm^{-1} ; ^1H NMR (300 MHz, CDCl₃): δ (ppm) 5.32 (s, 2H, CH₂), 6.55 (d, J = 16.0 Hz, 1H, CH=CH-CO), 7.35–7.51 (m, 8H, aromatic), 7.52–7.60 (m, 2H, aromatic), 7.80 (d, J = 16.0 Hz, 1H, CH=CH-CO); FAB MS m/z 239 (M+H)⁺.

4.3.12. (E)-Phenyl cinnamate (30). This compound was prepared from *trans*-cinnamic acid and phenol by method A, as slightly yellow crystals. Yield 75%; mp 72–75 °C, (lit.³⁸ mp 73.5–75.5 °C); IR (KBr): ν_{max} 3435, 2117, 1726, 1639, 1484, 1450, 1307, 1206, 1146, 970, 762, 680, and 552 cm^{-1} ; ^1H NMR (300 MHz, CDCl₃): δ (ppm) 6.67 (d, J = 16.0 Hz, 1H, CH=CH-CO), 7.17–7.32 (m, 3H, aromatic), 7.39–7.51 (m, 5H, aromatic), 7.58–7.66 (m, 2H, aromatic), 7.90 (d, J = 16.0 Hz, 1H, CH=CH-CO); FAB MS m/z 225 (M+H)⁺.

4.3.13. (E)-3-Phenoxyphenyl cinnamate (31). This compound was prepared from *trans*-cinnamic acid and (3-phenoxyphenyl)methanol by method B, as white crystals. Yield 84%; mp 48–51 °C; IR (KBr): ν_{max} 3038, 2942, 1713, 1638, 1583, 1484, 1450, 1378, 1312, 1250, 1218, 1166, 1074, 982, 804, 749, and 686 cm^{-1} ; ^1H NMR (300 MHz, CDCl₃): δ (ppm) 5.53 (s, 2H, CH₂), 6.52 (d, J = 16.0 Hz, 1H, CH=CH-CO), 6.96–7.21 (m, 6H, aromatic), 7.31–7.46 (m, 6H, aromatic), 7.50–7.60 (m, 2H, aromatic), 7.76 (d, J = 16.0 Hz, 1H, CH=CH-CO); FAB MS m/z 331 (M+H)⁺; Anal.

Calcd for $C_{22}H_{18}O_3$: C, 79.98; H, 5.49. Found: C, 80.42; H, 5.69.

4.3.14. (E)-4-Cyanophenyl cinnamate (32). This compound was prepared from *trans*-cinnamic acid and 4-cyanophenol by method B, as slightly yellow crystals. Yield 77%; mp 102–105 °C; IR (KBr): ν_{\max} 3062, 2232, 1744, 1632, 1496, 1307, 1220, 1127, 965; 762, 548 cm^{-1} ; 1H NMR (300 MHz, $CDCl_3$): δ (ppm) 6.64 (d, $J = 16.0$ Hz, 1H, $CH=CH-CO$), 7.31–7.39 (m, 2H, aromatic), 7.42–7.52 (m, 3H, aromatic), 7.58–7.67 (m, 2H, aromatic), 7.70–7.79 (m, 2H, aromatic), 7.92 (d, $J = 16.0$ Hz, 1H, $CH=CH-CO$); FAB MS m/z 250 (M+H)⁺; Anal. Calcd for $C_{16}H_{11}NO_2$: C, 77.10; H, 4.45; N, 5.62. Found: C, 77.01; H, 4.79; N, 5.39.

4.3.15. (E)-4-Acetamidophenyl cinnamate (33). This compound was prepared from *trans*-cinnamic acid and *N*-(4-hydroxyphenyl)acetamide by method B, as yellow crystals. Yield 61%; mp 196–199 °C, (lit.³⁹ mp 200–201 °C); IR (KBr): ν_{\max} 3357, 1720, 1676, 1638, 1545, 1408, 1316, 1154, 980, 857, 768, and 682 cm^{-1} ; 1H NMR (300 MHz, $CDCl_3$): δ (ppm) 2.20 (s, 3H, CH_3), 6.64 (d, $J = 15.8$ Hz, 1H, $CH=CH-CO$), 7.15 (d, $J = 9.0$ Hz, 2H, aromatic), 7.32 (s, 1H, NH), 7.41–7.49 (m, 3H, aromatic), 7.50–7.66 (m, 4H, aromatic), 7.89 (d, $J = 15.8$ Hz, 1H, $CH=CH-CO$); FAB MS m/z 282 (M+H)⁺.

4.3.16. (E)-3-Methoxyphenyl cinnamate (34). This compound was prepared from *trans*-cinnamic acid and 3-methoxyphenol by method A, as an oil.⁴⁰ Yield 79%; IR (KBr): ν_{\max} 2931, 2117, 1731, 1636 1608, 1592, 1490, 1450, 1309, 1265, 1201, 1141, 978, and 765 cm^{-1} ; 1H NMR (300 MHz, $CDCl_3$): δ (ppm) 3.84 (s, 3H, Ar–O– CH_3), 6.65 (d, $J = 15.8$ Hz, 1H, $CH=CH-CO$), 6.72–6.87 (m, 3H, aromatic), 7.26–7.49 (m, 4H, aromatic), 7.51–7.66 (m, 2H, aromatic), 7.90 (d, $J = 15.8$ Hz, 1H, $CH=CH-CO$); EI MS m/z 254 (M).

4.3.17. (E)-4-(Octanamido)phenyl cinnamate (35). This compound was prepared from *trans*-cinnamic acid and *N*-(4-hydroxyphenyl)octanamide by method A, as white crystals. Yield 56%; mp 127–130 °C; IR (KBr): ν_{\max} 3361, 3062, 2921, 1717, 1679, 1636, 1537, 1408, 1316, 1196, 989, 979, 859, 765, and 680 cm^{-1} ; 1H NMR (300 MHz, $CDCl_3$): δ (ppm) 0.91 (t, $J = 6.6$ Hz 3H, CH_3), 1.16–1.50 (m, 10H, 5 \times CH_2), 2.37 (t, $J = 2.4$ Hz, 2H, CO– CH_2), 6.64 (d, $J = 16.0$ Hz, 1H, $CH=CH-CO$), 7.10–7.19 (m, 2H, aromatic), 7.22 (s, 1H, NH), 7.39–7.65 (m, 7H, aromatic), 7.89 (d, $J = 16.0$ Hz, 1H, $CH=CH-CO$); FAB MS m/z 366 (M+H)⁺; Anal. Calcd for $C_{23}H_{27}NO_3$: C, 75.59; H, 7.45; N, 3.83. Found: C, 75.66; H, 7.71; N, 4.01.

4.3.18. (E)-Cyclohexyl cinnamate (36). This compound was prepared from *trans*-cinnamic acid and cyclohexanol by method A, as a colourless oil.⁴¹ Yield 77%; IR (KBr): ν_{\max} 2936, 2858, 2118, 1709, 1638, 1450, 1174, 1017, and 768 cm^{-1} ; 1H NMR (300 MHz, $CDCl_3$): δ (ppm) 1.05–2.10 (m, 11H, cyclohexyl) 6.46 (d,

$J = 16.0$ Hz, 1H, $CH=CH-CO$), 7.34–7.60 (m, 5H, aromatic), 7.69 (d, $J = 16.0$ Hz, 1H, $CH=CH-CO$); FAB MS m/z 231 (M+H)⁺.

4.3.19. Benzyl 2-oxo-2H-chromene-3-carboxylate (37). This compound was prepared from 2-oxo-2H-chromene-3-carboxylic acid and benzyl alcohol by method A, as white crystals. Yield 70%; mp 88–91 °C (lit.⁴² mp not given); IR (KBr): ν_{\max} 3053, 1760, 1698, 1619, 1568, 1455, 1307, 1215, 1001, 770, 641 cm^{-1} ; 1H NMR (300 MHz, $CDCl_3$): δ (ppm) 5.42 (s, 2H, CH_2), 7.26–7.70 (m, 9H, aromatic), 8.57 (s, 1H, $CH=C$); FAB MS m/z 281 (M+H)⁺.

4.3.20. (E)-2-(1,3-Dioxoisindolin-2-yl)ethyl 3-(3,4,5-trimethoxyphenyl)acrylate (38). This compound was prepared from (E)-3-(3,4,5-trimethoxyphenyl)acrylic acid and 2-(2-hydroxyethyl)isoindoline-1,3-dione by method B, as white crystals. Yield 75%; mp 118–120 °C; IR (KBr): ν_{\max} 2928, 2830, 1774, 1717, 1590, 1510, 1394, 1338, 1243, 1130, 1014, 840, and 720 cm^{-1} ; 1H NMR (300 MHz, DMSO- d_6): δ (ppm) 3.89 (s, 9H, 3 \times OCH_3), 4.07 (t, $J = 5.5$ Hz, 2H, CH_2), 4.47 (t, $J = 5.5$ Hz, 2H, CH_2), 6.30 (d, $J = 15.8$ Hz, 1H, $CH=CH-CO$), 6.75 (s, 2H, aromatic), 7.59 (d, $J = 15.8$ Hz, 1H, $CH=CH-CO$), 7.72–7.78 (m, 2H, aromatic), 7.85–7.94 (m, 2H, aromatic); FAB MS m/z 412 (M+H)⁺; Anal. Calcd for $C_{22}H_{21}NO_7$: C, 64.23; H, 5.15; N, 3.40. Found: C, 64.20; H, 5.32; N, 3.54.

4.3.21. (E)-Phenyl 3-(3,4,5-trimethoxyphenyl) acrylate (39). This compound was prepared from (E)-3-(3,4,5-trimethoxyphenyl)acrylic acid and phenol by method B, as white crystals. Yield 63%; mp 95–97 °C; IR (KBr): ν_{\max} 2937, 2836, 1725, 1581, 1508, 1456, 1417, 1340, 1240, 1184, 1127, 972, 931, 833, 725, and 640 cm^{-1} ; 1H NMR (300 MHz, DMSO- d_6): δ (ppm) 3.70 (s, 3H, OCH_3), 3.80 (s, 6H, 2 \times OCH_3), 6.91 (d, $J = 16.2$ Hz, 1H, $CH=CH-CO$), 7.12–7.32 (m, 2H, aromatic), 7.42–7.51 (m, 5H, aromatic), 7.81 (d, $J = 16.2$ Hz, 1H, $CH=CH-CO$); FAB MS m/z 315 (M+H)⁺; Anal. Calcd for $C_{18}H_{18}O_5$: C, 68.78; H, 5.77. Found: C, 68.43; H, 6.07.

4.3.22. (E)-Benzyl 3-(3,4,5-trimethoxyphenyl) acrylate (40). This compound was prepared from (E)-3-(3,4,5-trimethoxyphenyl)acrylic acid and benzyl alcohol by method B, as yellowish white crystals. Yield 68%; mp 88–89 °C, (lit.⁴³ 87–89 °C); IR (KBr): ν_{\max} 2958, 1704, 1638, 1582, 1505, 1418, 1275, 1128, 1002, 827, 756, 691, and 620 cm^{-1} ; 1H NMR (300 MHz, DMSO- d_6): δ (ppm) 3.69 (s, 3H, OCH_3), 3.81 (s, 6H, 2 \times OCH_3), 6.72 (d, $J = 16.2$ Hz, 1H, $CH=CH-CO$), 7.09 (s, 2H, aromatic), 7.47–7.56 (m, 5H, aromatic), 7.63 (d, $J = 16.2$ Hz, 1H, $CH=CH-CO$); FAB MS m/z 329 (M+H)⁺.

4.3.23. (E)-1-Naphthyl 3-(3,4,5-trimethoxy phenyl) acrylate (41). This compound was prepared from (E)-3-(3,4,5-trimethoxyphenyl)acrylic acid and 1-naphthol by method B, as brownish white crystals. Yield 55%; mp 131–134 °C; IR (KBr): ν_{\max} 1707, 1579, 1503, 1418, 1339, 1225, 1120, 990, 835, and 780 cm^{-1} ; 1H NMR

(300 MHz, DMSO- d_6): δ (ppm) 3.74 (s, 3H, OCH₃), 3.86 (s, 6H, 2× OCH₃), 7.10 (d, $J = 15.9$ Hz, 1H, CH=CH–CO), 7.24 (s, 2H, aromatic), 7.40 (d, $J = 6.6$ Hz, 1H, aromatic), 7.55–7.66 (m, 3H, aromatic), 7.87–7.90 (m, 2H, aromatic), 7.93 (d, $J = 15.9$ Hz, 1H, CH=CH–CO), 7.93–8.03 (m, 1H, aromatic); FAB MS m/z 365 (M+H)⁺; Anal. Calcd for C₂₂H₂₀O₅·0.25H₂O: C, 71.63; H, 5.60. Found: C, 71.84; H, 5.65.

4.4. Construction of a QSAR model

Three-dimensional structures of the molecules in the data set were generated by SPARTAN 5.0 software.⁴⁴ After initial crude minimization, a multiple conformational search was performed using the Monte Carlo method, in connection with simulated annealing. These geometries were imported into the MOPAC program package.⁴⁵ The AM1 semi-empirical approach was used and the effect of solvation was taken into account. We analyzed the resulting conformers, and the structures with the corresponding lowest solvation energies were used for quantum-chemical descriptors' calculation by the CODESSA program package.^{46,47}

CODESSA (comprehensive descriptors for structural and statistical analysis) is a multipurpose program for developing quantitative structure–activity structure–property relationships (QSARs/QSPRs). It provides various methods for statistical analysis of experimental data, such as linear and non-linear regression, principal component analysis (PCA) and non-linear iterative partial least squares (NIPALS). A set of 640 molecular descriptors derived from geometrical and quantum-chemical information was generated for each molecular structure.

The measurements of inhibitory activity against fungal 17 β -hydroxysteroid dehydrogenase were conducted for 41 and 39 compounds for the directions of oxidation and reduction, respectively. The IC₅₀ values for compounds **27** and **28** for the inhibition of reduction were not available. Compound **37** appeared to be an outlier (its cross-validated residual ~ 3 was more than 3×RMS error prediction value) in all constructed QSAR models and was therefore not included in the QSAR model. Thirteen out of 39 compounds determined for the reduction direction were inactive and their inhibitory activities were set to an arbitrary IC₅₀ of 3000 μ M. In order to address the question of arbitrarily chosen upper limit for the inactive compounds, we have also performed the following experiment (for oxidation and reduction part of the reaction): in a series of inactive compounds the value 3 mM (value on a log scale is 2.568) was substituted for 1 mmol (value on a log scale is 3) and the best linear model sought for. The variation of the final model obtained was negligible. Thus, it was shown no significant error was introduced by using arbitrarily chosen value of 3 mM for the upper limit of concentration of inactive compounds and simultaneously assuring that the binding to the enzyme is marginal.

To develop meaningful QSAR models that could be validated on an independent set of ligands, we randomly divided our initial sets of 40 (oxidation direction) and

36 (reduction direction) compounds into four subsets. Different combinations of three subsets consisting of 11 (oxidation) or 10 (reduction) were used as training and test sets (33 or 30 molecules). The remaining seven compounds in the case of oxidation and six compounds in the case of reduction comprised external prediction (validation) sets. Similarly, from the set of inactive molecules, two (**24** and **34**) were selected at random and placed in the external prediction set for subsequent validation of the oxidation model. Analogously, two inactive molecules (**19** and **32**) were randomly selected and excluded in the building of the reductive QSAR model. The compounds were distributed into these three sets in a completely random fashion thus ensuring independent external validation.

We were careful to limit the number of inactives to <1/3 of the total number of compounds in the data set. We believe that the prediction ability of the model which was carefully designed and is based on the division of the data set into training, test and external prediction (validation) set is useful.

QSAR models were developed following a standard procedure. First, a training set was used to obtain four molecular descriptors present in the QSAR equation by the best multiple linear regression (BMLR) algorithm. In this procedure, the orthogonal descriptors are added to the model, successively starting with the best pair of descriptors in the first step. In the next step, descriptor triples were chosen that obeyed Fisher criterion F at a given probability level (a detailed description can be found in Ref. 46).

Furthermore, another subset (11 or 10 compounds) was added, and with previously determined descriptors, a new QSAR model was calculated using the multiple linear regression (MLR) procedure. Finally, a cross-validated correlation coefficient r_{cv}^2 (CV-LOO) was calculated on a joint set. The procedure was repeated twice, and the model with the highest value of r_{cv}^2 was finally accepted.

The BMLR algorithm was used because of it can be used to obtain QSAR equations, which consist solely of orthogonal descriptors with inter-descriptor correlations less than 0.4000.⁴⁸ By setting the parameters of the BMLR procedure appropriately (max r^2 for orthogonal scales = 0.25, and max r^2 for collinear scales = 0.25), the resulting equations consisted of orthogonal descriptors with no overlap of information.

4.5. Molecular docking into the active site

The FlexX molecular docking tool incorporated into a Sybyl framework was used for this evaluation.⁴⁹ The substrate androstenedione included in the homology model was taken as a reference structure and the area 10 Å around it was considered as the active site. The potent flavone **1** and *trans*-cinnamic acid ester **29** were chosen as representative structures. The proposed 30 binding modes of the docked inhibitors were evaluated using RMS as a tool to explore relative structural

differences between proposed binding modes. The graphical representations of the proposed binding positions of molecules **1** and **29** were obtained using Insight II molecular modelling environment.⁵⁰

The human 17 β -HSD1 enzyme was obtained from the Brookhaven database of protein structures (PDB code: 1A27).

4.6. Inhibition studies

Compounds were tested for their inhibitory activities towards homogeneous recombinant 17 β -HSDcl. 17 β -HSDcl catalyzes oxidation of 4-estrene-17 β -ol-3-one to 4-estrene-3,17-dione in the presence of NADP⁺, and reduction of 4-estrene-3,17-dione to 4-estrene-17 β -ol-3-one in the presence of coenzyme NADPH. The reaction was followed spectrophotometrically by measuring the difference in NADPH absorbance ($\epsilon_{\lambda 340} = 6270 \text{ M}^{-1} \text{ cm}^{-1}$) in the absence and presence of the compounds.^{23,25} Assays were carried out in a 0.6-ml volume in 100 mM phosphate buffer (pH 8.0) containing 1% DMSO as co-solvent, as described previously.^{23,25} The concentrations of substrate and coenzyme were 100 μM each, and the compounds were tested from 0.01 to 100 μM ; the enzyme was 0.5 μM . Initial velocities of enzymatic reactions in the absence (v_0) or presence (v_i) of inhibitor were measured. Percentage inhibition (% inh.) was given by $100 - ((v_i/v_0) \times 100)$. IC₅₀ values were determined graphically from plots of % inh. versus log (inhibitor concn) using GraphPad Prism Version 4.00 (GraphPad Software, Inc.). Control experiments according to Shoichet's methodology⁵¹ in the presence of 0.01% (v/v) Triton X-100 were performed for five selected compounds (**24**, **29**, **30**, **32**, and **37**) that were active in high, medium and low micromolar IC₅₀ range in order to exclude non-specific binding of inhibitors. No significant differences were found when compared to measurements without Triton X-100.

Acknowledgments

This work was supported financially by the Ministry of Education, Science and Sport of the Republic of Slovenia. The authors thank Professor Dr. Roger Pain for critical reading of the manuscript.

References and notes

- Penning, T. M. *Endocr. Rev.* **1997**, *18*, 281.
- Mindnich, R.; Möller, G.; Adamski, J. *Mol. Cell. Endocrinol.* **2004**, *218*, 7.
- Lukacik, P.; Kavanagh, K. L.; Oppermann, U. *Mol. Cell. Endocrinol.* **2006**, *248*, 61.
- Bros, W.; Heller, W.; Michel, C. In *Flavonoids in Health and Disease*; Rice-Evans, C. A., Packer, L., Eds.; Marcel Dekker: New York, 1998; pp 111–136.
- Middelton, E., jr.; Kandaswami, C.; Theoharides, T. C. *Pharmacol. Rev.* **2000**, *52*, 673.
- Tham, D. M.; Christopher, D.; Gardner, D.; Haskell, W. L. *J. Clin. Endocrinol. Metab.* **1998**, *83*, 2223.

- Osocki, A. L.; Kennelly, E. J. *Phytother. Res.* **2003**, *17*, 845.
- Le Bail, J.-C.; Champavier, Y.; Chulia, A.-J.; Habrioux, G. *Life Sci.* **2000**, *66*, 1281.
- Kirk, C. J.; Harris, R. M.; Wood, D. M.; Waring, R. H.; Hughes, P. J. *Biochem. Soc. Trans.* **2001**, *29*, 209.
- Ohno, S.; Matsumoto, N.; Watanabe, M.; Nakajin, S. *J. Steroid Biochem. Mol. Biol.* **2004**, *88*, 175.
- Ohno, S.; Shinoda, S.; Toyoshima, S.; Nakazawa, H.; Makino, T.; Nakajin, S. *J. Steroid Biochem. Mol. Biol.* **2002**, *80*, 355.
- Lephart, E. D.; Lund, T. D.; Horvath, T. L. *Brain Res. Rev.* **2001**, *37*, 25.
- Weber, K. S.; Jacobson, N. A.; Setchell, K. D.; Lephart, E. D. *Proc. Soc. Exp. Biol. Med.* **1999**, *221*, 131.
- Schweizer, R. A.; Atanasov, A. G.; Frey, B. M.; Odermatt, A. *Mol. Cell. Endocrinol.* **2003**, *212*, 41.
- Le Lain, R.; Nicholls, P. J.; Smith, H. J.; Mahrlouie, F. H. *J. Enzyme Inhib.* **2001**, *16*, 35.
- Le Lain, R.; Barrell, K. J.; Saeed, G. S.; Nicholls, P. J.; Simons, C.; Kirby, A.; Smith, H. J. *J. Enzyme Inhib.* **2002**, *17*, 93.
- Le Bail, J.-C.; Pouget, C.; Fagnere, C.; Basly, J.-P.; Chulia, A.-J.; Habrioux, G. *Life Sci.* **2001**, *68*, 751.
- Makela, S.; Poutanen, M.; Lehtimaki, J.; Kostian, M.-L.; Santii, R.; Vihko, R. *Proc. Soc. Exp. Biol. Med.* **1995**, *208*, 51.
- Makela, S.; Poutanen, M.; Kostian, M. L.; Lehtimaki, N.; Strauss, L.; Santii, R.; Vihko, R. *Proc. Soc. Exp. Biol. Med.* **1998**, *217*, 310.
- Krazeisen, A.; Breitling, R.; Moeller, G.; Adamski, J. *Mol. Cell. Endocrinol.* **2001**, *171*, 151.
- Krazeisen, A.; Breitling, R.; Moeller, G.; Adamski, J. *Adv. Exp. Med. Biol.* **2002**, *505*, 151.
- Poirier, D. *Curr. Med. Chem.* **2003**, *10*, 453.
- Kristan, K.; Krajnc, K.; Konc, J.; Gobec, S.; Stojan, J.; Lanišnik Rižner, T. *Steroids* **2005**, *70*, 626.
- Heller, W.; Forkmann, G. In *The Flavonoids. Advances in Research since 1986*; Harborne, J. D., Ed.; Chapman and Hall Ltd.: London, 1993; pp 499–535.
- Gobec, S.; Sova, M.; Kristan, K.; Lanišnik Rižner, T. *Bioorg. Med. Chem. Lett.* **2004**, *14*, 3933.
- Oblak, M.; Randic, M.; Solmajer, T. *J. Chem. Inf. Comput. Sci.* **2000**, *40*, 994.
- (a) Greene, T. W.; Wuts, P. G. M. *Protective Groups in Organic Synthesis*, 2nd Ed.; John Wiley and Sons: New York, 1991; (b) Kocienski, P. J. *Protecting Groups*; Georg Thieme: Stuttgart, 1994.
- Castro, B.; Evin, G.; Selve, C.; Seyer, R. *Synthesis-Stuttgart* **1977**, *6*, 413.
- Lanišnik Rižner, T.; Moeller, G.; Thole, H. H.; Žakelj-Mavrič, M.; Adamski, J. *Biochem. J.* **1999**, *337*, 425.
- Allan, G. M.; Lawrence, H. R.; Cornet, J.; Bubert, C.; Fischer, D. S.; Vicker, N.; Smith, A.; Tutill, H. J.; Purohit, A.; Day, J. M.; Mahon, M. F.; Reed, M. J.; Potter, B. V. *J. Med. Chem.* **2006**, *49*, 1325.
- Deluca, D.; Moller, G.; Rosinus, A.; Elger, W.; Hillisch, A.; Adamski, J. *Mol. Cell. Endocrinol.* **2006**, *248*, 218.
- Kotnik, M.; Oblak, M.; Humljan, J.; Gobec, S.; Urleb, U.; Solmajer, T. *QSAR Comb. Sci.* **2004**, *23*, 399.
- Solmajer, T.; Zupan, J. *Drug Disc. Today Technol.* **2004**, *1*, 247.
- Homology model of 17- β HSDcl was downloaded from the web site: <<http://www2.mf.uni-lj.si/~stojan/stojan/html/>>.
- Cassetta, A.; Budefeld, T.; Rizner, T. L.; Kristan, K.; Stojan, J.; Lamba, D. *Acta Crystallogr. Sect. F* **2005**, *61*, 1032.
- Oppermann, U.; Filling, C.; Hult, M.; Shafgat, N.; Wu, X.; Lindh, M.; Shafqat, J.; Nordling, E.; Kallberg, Y.

- Persson, B.; Jörnvall, H. *Chem. Biol. Interact.* **2003**, *143/144*, 247.
37. Kunishima, M.; Kawachi, C.; Morita, J.; Terao, K.; Iwasaki, F.; Tani, S. *Tetrahedron* **1999**, *55*, 13159.
38. Fuson, R. C.; Thomas, N. *J. Org. Chem.* **1953**, *18*, 1762.
39. Dittert, L. W.; Caldwell, H. C.; Adams, H. J.; Irwin, G. M.; Swintosky, J. V. *J. Pharm. Sci.* **1968**, *57*, 774.
40. Krajniak, E. R.; Ritchie, E.; Taylor, W. C. *Aust. J. Chem.* **1973**, *26*, 899.
41. Akai, S.; Tsuzuki, Y.; Satoshi, M.; Kitagaki, S.; Kita, Y. *J. Chem. Soc., Perkin Trans. 1* **1992**, 2813.
42. Orita, M.; Yamamoto, S.; Katayama, N.; Motonori, A.; Takayama, K.; Yamagiwa, Y.; Seki, N.; Suzuki, H.; Kurihara, H.; Sakashita, H.; Takeuchi, M.; Fujita, S.; Yamada, T.; Tanaka, A. *J. Med. Chem.* **2001**, *44*, 540.
43. Ulibarri, G.; Choret, N.; Bigg, D. C. H. *Synthesis* **1996**, 1286.
44. Spartan 5.0 Wavefunction. In Irvine, CA, USA.
45. Steward, J. J. P. MOPAC 93 annual revision Number 2, Fujitsu **1993**.
46. Katritzky, A.; Lobanov, V. S.; Karelson, M. CODESSA, Reference manual, Gainesville, 1995.
47. Katritzky, A.; Lobanov, V. S.; Karelson, M. CODESSA, Training manual, Gainesville, 1995.
48. Topliss, J. G.; Costello, R. J. *J. Med. Chem.* **1972**, *15*, 1066.
49. Sybyl 7.0, Tripos software, St. Louis, USA.
50. Insight II, Accelrys software, San Diego, CA, USA.
51. McGovern, S.; Helfand, B. T.; Feng, B.; Shoichet, B. K. *J. Med. Chem.* **2003**, *46*, 4265.